

Lawrence Berkeley National Laboratory

Recent Work

Title

CROSSED BEAMS CHEMISTRY: REACTIONS OF Ba, Sr, Ca, AND Mg WITH Cl₂ AND Br₂

Permalink

<https://escholarship.org/uc/item/4pc0w2fx>

Authors

Lin, Shen-Maw
Mims, Charles A.
Herm, Ronald R.

Publication Date

1972-08-01

CROSSED BEAMS CHEMISTRY:
REACTIONS OF Ba, Sr, Ca,
AND Mg WITH Cl₂ AND Br₂

Shen-Maw Lin, Charles A. Mims
and Ronald R. Herm

August 1972

AEC Contract No. W-7405-eng-48

TWO-WEEK LOAN COPY

*This is a Library Circulating Copy
which may be borrowed for two weeks.
For a personal retention copy, call
Tech. Info. Division, Ext. 5545*



DISCLAIMER

This document was prepared as an account of work sponsored by the United States Government. While this document is believed to contain correct information, neither the United States Government nor any agency thereof, nor the Regents of the University of California, nor any of their employees, makes any warranty, express or implied, or assumes any legal responsibility for the accuracy, completeness, or usefulness of any information, apparatus, product, or process disclosed, or represents that its use would not infringe privately owned rights. Reference herein to any specific commercial product, process, or service by its trade name, trademark, manufacturer, or otherwise, does not necessarily constitute or imply its endorsement, recommendation, or favoring by the United States Government or any agency thereof, or the Regents of the University of California. The views and opinions of authors expressed herein do not necessarily state or reflect those of the United States Government or any agency thereof or the Regents of the University of California.

-iii-

CROSSED BEAMS CHEMISTRY:

REACTIONS OF Ba, Sr, Ca, AND Mg WITH Cl₂ AND Br₂Shen-Maw Lin*, Charles A. Mims[†], and Ronald R. Herm

Inorganic Materials Research Division,
Lawrence Berkeley Laboratory and Department of Chemistry,
University of California, Berkeley, California 94720

ABSTRACT

Reactions of Ba, Sr, Ca, and Mg with Cl₂ and Br₂ have been studied in a crossed beam apparatus employing an electron bombardment ionizer-massfilter detector. Product center-of-mass (CM) recoil energy and angle distributions have been fit to the measured monohalide product (MX) laboratory (LAB) angular distributions by averaging the CM→LAB transformations over the measured (non-thermal) beam speed distributions. These experiments give no indications of a dihalide product (MX₂) and indicate that the formation of MX₂ (by a two-body radiative association) cannot account for more than a small fraction (< ~ 5%) of the reactive collisions. All eight reactions favor forward product scattering (i.e., MX scattered in the direction defined by the incident M)

* Present address: Department of Theoretical Chemistry, Cambridge University, Cambridge, CB2 1EW, England.

† Present address: Department of Chemistry, Massachusetts Institute of Technology, Cambridge, Massachusetts.

with relatively low recoil energies ($\sim 10-20\%$ of the reaction exoergicity). For reaction with either halogen molecule, the fraction of the product scattered into the forward CM hemisphere increases in the sequence: Mg, Ca, Sr, Ba. Similarities and differences between the results of the present study and features of the reactions of alkali atoms are discussed.

In recent years, crossed beam studies¹ have indicated that the reactions of the alkali atoms with halogen molecules are characterized by large reactive cross sections, Q_R , high internal excitation of the products, and a product alkali halide angular distribution which is sharply peaked forward (i.e., in the direction defined by the incoming alkali atom). Although it fails to account quantitatively for the magnitude of Q_R in the $M + I_2$ reactions², these features have been rationalized qualitatively in terms of a simple electron transfer model. This model pictures a transfer of the alkali atom valence electron to the halogen molecule at a distance of reactant approach, r_c , estimated in terms of the atom ionization potential, $I(M)$, and halogen electron affinity, $E(X_2)$, by $r_c = e^2 / (I(M) - E(X_2))$. The reaction is then pictured as proceeding via the breakup of the X_2^- ion to give the ionically bound alkali halide product, i.e., $M + X_2 \rightarrow M^+ \cdots X_2^- \rightarrow M^+ X^- + X$.

The introduction of the electron bombardment ionizer-mass spectrometer universal detector within the last few years has vastly extended the chemical scope of crossed beam studies of neutral reactions. This has prompted a number of studies^{3,4} of the reactions of Group IIA alkaline earth atoms. This paper reports results on the reactions of Ba, Sr, Ca, and Mg with Cl_2 and Br_2 .

The study of this family of reactions should complement and extend the evolving picture of the dynamics of alkali atom reactions because of interesting similarities and differences between the alkali and alkaline earth atoms. Thus, although Ba does not possess an unpaired spin, the electron transfer model suggests that it should react rapidly with halogen molecules because its ionization potential is actually less than that of the Li atom (5.2 vs. 5.4 ev.). The ionization potential of the Mg atom, on the other hand, is too large (7.6 ev.) to realistically picture its reactions as proceeding via an intermediate $Mg^+ - X_2^-$ ionic configuration. Another interesting difference between the two families of reactions arises because the stability of the alkaline earth dihalides gives rise to a deep chemical well in the potential hypersurface for the alkaline earth reactions which is not present in that for the alkali reactions. The presence of this well could result in longer collision lifetimes and a broadening of the product angular distribution; some indications of longer collision lifetimes are suggested by the recent observation⁵ of the two-body radiative attachment of Ba and Sr to Cl_2 .

EXPERIMENTAL PROCEDURE

The apparatus is described in detail in Ref. 6. The detector, housed in a differentially-pumped UHV chamber and able to see the entire beam collision zone, may be rotated about the collision zone, in the plane defined by the two intersecting beams, so as to scan a range of laboratory (LAB) scattering angles, θ , from

-15° to +115°; Fig. 1 illustrates that $\theta = 0^\circ$ is defined by the incident M direction, $\theta = 90^\circ$ by the incident X_2 direction. The scattered species are ionized by ~ 150 eV electrons, mass analyzed, and detected, via electron multiplier amplification, by means of a PAR HR-8 lock-in amplifier referenced (with negligible phase shift) to the halogen beam modulation frequency (typically 43 Hz square wave modulation). All of the product angular distribution measurements reported here were obtained with the mass spectrometer tuned to the MX^+ signal. Although the neutral precursor of this ion might be either MX or MX_2 , arguments presented in a later section indicate that it arose predominately (if not exclusively) from ionization of MX. Although careful mass scans were made for some of the scattering partners (notably Ba and Mg with Cl_2 and Br_2), no scattered signals have been observed at the MX_2^+ mass peaks. The Sr^+ angular distribution of scattering of Sr off of Br_2 was also measured; its behavior was similar to that of the non-reactive scattering of alkali atoms from Br_2 at narrow angles, but it fell off less rapidly at larger scattering angles. However, some of this Sr^+ signal might have arisen from ionization of SrBr rather than Sr; this possibility precludes any inferences regarding the elastic scattering in the collisions studied here. This inability to study the elastic scattering as well as unknown detector response factors also precludes the determination of total reaction cross sections; order-of-magnitude estimates suggest $Q_R \sim 10-100 \text{ \AA}^2$ for Ba + Br_2 and Q_R for Mg reactions about 25% of those for Ba reactions. Jonah and Zare⁵ reported $Q_R = 60 \text{ \AA}^2$ for Ba + Cl_2 .

The halogen molecule beam emerges from a "crinkly-foil" many-channel source, 0.16 cm wide \times 0.7 cm high, prepared by stacking alternate layers of flat and corrugated (0.01 cm corrugation width) stainless steel foil (0.0025 cm thick \times 0.7 cm high \times 0.5 cm wide). Although this beam source is situated in the collision chamber, background pressures were $\lesssim 10^{-6}$ Torr (uncorrected ion gauge reading). Measurements of the halogen beam number density probability speed distributions showed them to be appreciably non-thermal and well fit by the empirical function

$$\rho_2(v_2) = N_2 (v_2 - a_2)^2 \exp[-(v_2 - a_2)^2 / \alpha_2^2] u(v_2 - a_2). \quad (1)$$

Here, $u(t)$ is the unit step function ($u(t)=0$ for $t \leq 0$, $u(t)=1$ for $t > 0$); α_2 is the most probable thermal speed in the source ($\alpha_2 = (2kT_2/M_2)^{1/2}$); $N_2 = 4\pi^{-1/2} \alpha_2^{-3}$; and a_2 is a "flow speed" which increases with increasing source pressure.

The alkaline earth atoms emerge from a knife-edge slit (0.05 cm wide \times 0.5 cm high) in a resistively-heated, single chamber stainless steel oven. After collimations, the two beams intersect at right angles resulting in a 1-5% attenuation of the M beam and negligible attenuation of the X_2 beam. Measurements of the Ba beam speed distribution showed far less deviation from thermal behavior than was found for the halogen beams, although the low speed tail of the thermal distribution was appreciably attenuated. The approximate theory of deviations from thermal speed distributions due to intrabeam collisions which is developed in Ref. 7 predicts the same percent deviation as a function of reduced speed

(true speed divided by most probable thermal source speed) for two gases with the same collision cross section. Consequently, the thermal attenuation factors measured for the Ba beam were applied to the Sr, Ca, and Mg beam speed distributions. This procedure should adequately estimate^{6a} the unmeasured Sr, Ca, and Mg speed distributions, although it may slightly overestimate the non-thermal behaviors due to decreasing collision cross sections. Empirically, the alkaline earth number density probability speed distributions, $\rho_1(v_1)$, are also well fit by Eq.(1); in this case, however, both a_1 and α_1 are functions of the source pressure.

Figure 1 shows the angular profiles of the two beams and Table I lists beam operating conditions. All of the data analysis which is presented in the following section included averages over the actual beam speed distributions. Auxiliary calculations for thermal beams indicated that the derived center-of-mass (CM) cross section results could be considerably in error if the true halogen beam speed distributions had not been used; on the other hand, recognition of the smaller deviations from thermal behavior of the alkaline earth beams had much less influence on the derived CM cross sections.

DATA ANALYSIS AND RESULTS

Figure 1 shows a diagram of the LAB \leftrightarrow CM transformation for the $\text{Ba} + \text{Cl}_2 \rightarrow \text{BaCl} + \text{Cl}$ reaction; the CM scattering angle, θ , is defined as 0° when the BaCl CM recoil velocity, \vec{u} , lies along the initial relative velocity vector, \vec{V} , in the direction defined

by the incident Ba; the LAB velocity of the center-of-mass of the collision partners, \vec{C} , is also shown. Figures 1-3 show that the measured LAB product angular distributions all peak at smaller LAB angles than do the distributions in \vec{C} (calculated³ assuming an energy independent collision cross section); furthermore, the data points fall off smoothly with angle through the angular regions of the peaks in the \vec{C} distributions. Since any MX_2 product formed must recoil in the LAB along \vec{C} , these comparisons show that the MX^+ measured signal must arise primarily from ionization of an MX product which has scattered predominately forward in the CM coordinate system. Jonah and Zare⁵ estimate that the two-body radiative association of Ba to Cl_2 which they observe accounts for only a small fraction of reactive encounters for these collision partners. The present experiment should be especially sensitive to any MX_2 which formed because it would be solely confined to the detector-scan plane. A simple calculation, based on the smooth fall-off of the measured data through the angular ranges of the peaks of the \vec{C} distributions, indicates that MX_2 formation cannot account for as much as 1-5% of the reactive encounters for the collision partners studied in this work.

The measured MX LAB number density angular distribution is related (in arbitrary units) to the CM reactive cross section, $\sigma(\theta, u)$, by

$$I_{\text{LAB}}(\theta) = \iiint_0^\infty v \sigma(\theta, u) (v/u^2) \rho_1(v_1) \rho_2(v_2) dv_1 dv_2 dv \quad (2)$$

where v and u are the LAB and CM recoil speeds of MX. In analyzing

the data by means of Eq.(2), it is assumed that $\sigma(\theta,u)$ is independent of relative velocity, V . Although Whitehead, Hardin, and Grice⁸ have recently reported some differences between their higher energy (~ 5 kcal/mole) results on the $K + Br_2$ reaction and earlier thermal energy studies, the validity of this assumption is strongly supported by recent very careful measurements on the $K + I_2$ reaction.⁹ These measurements indicated that an increase in collision energy from 1.9 to 3.6 kcal/mole produces only slight changes in the magnitude and shape of the $K + I_2$ CM reactive cross section. A second assumption of the data analysis procedure employed here is the separability of the CM recoil energy and angle distributions, i.e.

$$\sigma(\theta,u) = T(\theta) U(u). \quad (3)$$

Here again, this assumption is supported by the careful study⁹ of the $K + I_2$ reaction which indicated only a weak coupling of these two distributions.

The actual data analysis procedure consist in assuming a form for $T(\theta)$ and $U(u)$ and calculating the resultant LAB angular distribution for comparison with the experimental data; this is repeated until a good fit to the data is achieved. Owing to the inability of the present experiments to measure the distribution in LAB recoil velocities and the resultant integration over v indicated in Eq.(2), a number of $T(\theta)$ and $U(u)$ combinations will often fit the data measured for a given reaction. In order to provide insight into the $T(\theta)$ and $U(u)$ functions compatible with the data, two different extreme data analyses are presented for

each reaction. The first, denoted the "stochastic" result, employs $T(\theta)$ and $U(u)$ functions of the form¹⁰

$$T(\theta) = (1-C_1) \exp\{-\ln 2((\theta-\theta_1)/H_1)^2\} + C_1, \text{ and} \quad (4a)$$

$$U(u) = (u/u_1)^{n_1} \exp\{(n_1/m_1)(1-(u/u_1)^{m_1})\}, \quad u < u_1$$

$$U(u) = 1, \quad u_1 \leq u \leq u_2, \text{ and} \quad (4b)$$

$$U(u) = (u/u_2)^{n_2} \exp\{(n_2/m_2)(1-(u/u_2)^{m_2})\}, \quad u > u_2$$

where all subscripted variables serve as adjustable parameters.

The stochastic procedure employed here uses these functions to obtain the $T(\theta)$ function with the narrowest breadth of the forward scattered component (i.e., smallest H_1 value) which will provide a good fit (i.e., within the estimated uncertainty of the data points) over the entire angular range of the measured data.

Figures 1-3 indicate that this procedure provided good fits for all eight reactions studied here; these fits were all obtained with $u_1=u_2$ and $n_1=n_2=m_1=m_2=2$ in Eq. (4b). The $T(\theta)$ functions which provided these good fits are shown in Figures 1, 4, and 5, and Table II lists the parameters of the $T(\theta)$ and $U(u)$ functions. Figure 1 also shows the distribution in translational recoil energy, E' , with which the BaCl and Cl products of the Ba + Cl₂ reaction separate; this is obtained from the $U(u)$ function by $P(E')dE' = U(u)du$.

The second data analysis extreme, denoted the "Single Recoil Energy" (SRE) result, proceeds by assuming that the MX product is scattered with a single, fixed CM recoil speed. Since this

procedure removes the flexibility in the $U(u)$ function of Eq. (4b), the $T(\theta)$ function has not been restricted to the form of Eq. (4a) in seeking fits to the measured LAB data. Because the full breadth of the measured LAB angular distribution must be accounted for by the $T(\theta)$ function, the SRE result should provide an upper limit to the overall breadth of the true CM angular distribution. Derived SRE CM angular distributions are shown in Figs. 1, 4, and 5 and Table II lists the derived single product recoil energies. Figures 1-3 indicate that the SRE procedure failed to provide a good fit to the measured data for some of the reactions.

In general, data on any reactions which are adequately fit by the SRE analysis could also be fit by a family of $T(\theta)$ functions bounded by the extremes presented in Figs. 4 or 5. In practice, however, the true CM angular distribution should be closer in shape to the stochastic extreme because product velocity measurements on the analogous $K + I_2^9$ and $K + Br_2^{12}$ reactions indicate product recoil energy distributions which are of quantitatively similar shape to the stochastic results presented here. Results of calculations for a variety of $T(\theta)$ functions in combination with the flexible $U(u)$ function given in Eqs. (4a) and (4b) have also provided the following further constraints on the form of the true CM angular distribution for all of the reactions studied here: (1) any $T(\theta)$ symmetric about $\theta = 90^\circ$ is incompatible with the data; (2) $T(\theta)$ must peak at $\theta \leq 20^\circ$; (3) there is substantial MX scattered intensity beyond 90° , arbitrarily provided here, in the stochastic analysis, by an isotropic component; and (4) $T(\theta)$ might actual have a secondary peak at 180° , but it cannot

be larger than ~30% of the forward peak intensity. Figure 1 illustrates points (2) and (4) for the Ba + Cl₂ reaction. A recent study of the Ba + Cl₂ reaction reported⁴ a BaCl angular distribution spanning a range of LAB angles from -25° to ~60°; this was fit to CM cross sections which are qualitatively quite similar to the stochastic results shown in Fig. 1. Quantitatively, however, the CM cross sections reported in Ref. 4 do not fit the data points shown in Fig. 1 as well as the stochastic or SRE fits obtained here, especially at wide LAB angles where they predict insufficient scattered intensity.

Owing to the Jacobian factor in Eq. (2), the measured LAB data is relatively insensitive to the form of U(u) at high recoil speeds so that not too much significance should be assigned to the stochastic forms of U(u) given in Fig. 1 and Table II. However, the most probable product recoil energies, derived from the peaks in the P(E') functions, should be approximately true because, as Table II indicates, these derived values are approximately constant for very different assumptions (stochastic vs. SRE) regarding the form of P(E').

DISCUSSION

Table III lists the fraction of the MX product scattered into the forward hemisphere,

$$Q_F = \int_0^{\pi/2} T(\theta) \sin\theta d\theta / \int_0^{\pi} T(\theta) \sin\theta d\theta.$$

Although present to some extent in the SRE results as well, the following trends in Q_F evaluated from the more reliable stochastic

results are apparent: (1) for a given alkaline earth atom, the Cl_2 reaction produces somewhat more forward scattering than does the Br_2 reaction; (2) for a given X_2 , the forward MX scattered component increases in the sequence Mg, Ca, Sr, Ba; and (3) Sr + Br_2 more closely resembles Ca + Br_2 whereas Sr + Cl_2 more closely resembles Ba + Cl_2 . The first two trends are also observed in the reactions of the alkali atoms with halogen molecules.¹ The third trend correlates with the geometries (linear vs. bent) of the ground electronic states of the alkaline earth dihalides, although it is not clear how much significance should be assigned to this correlation because of the many other uncertain parameters associated with these reactions (e.g., precise forms of $T(\theta)$, reliable values for $D_0(\text{MBr})$, and the absence of trajectory studies).

Quantitative comparisons of the present results with published results for the alkali atom reaction could be misleading because (1) the study reported here has not uniquely determined the forms of the CM cross sections and (2) results for most of the alkali reactions have been analyzed by a procedure, similar to the SRE procedure employed here, which assumed thermal beam speed distributions. The similarity of the ^{present} stochastic results for Ba + Br_2 to the accurate CM cross sections for K + Br_2 ¹² was pointed out in the previous section. It is also clear from the data presented here that the Ba atom reactive cross sections are qualitatively much more similar to those of the Cs reactions^{13,14} rather than the Li reactions.¹⁵ This observation is somewhat surprising because the electron transfer model would suggest that Li and Ba are likely to react within a similar range of impact

parameters; it may indicate a high sensitivity of the product angular distributions in these electron transfer reactions to the mass of the attacking atom. Existing trajectory calculations^{16,17} do not support this conjecture, although these calculations have not extensively studied the influence of changing reactant masses.

In view of the deep chemical wells in the potential hypersurfaces for the alkaline earth reactions which are associated with the stability of the alkaline earth dihalides, this similarity between the reactions of alkali atoms and the heavier alkaline earth atoms (notably Ba) is striking. Studies of the reactions of alkali atoms with alkali halides¹⁸ clearly indicate that the presence of a well corresponding to a stable intermediate can result in a long-lived collision complex reaction mechanism; on the other hand, the direct product scattering observed in the $\text{Li} + \text{NO}_2$ reaction¹⁹ indicates that this need not always be true. Co-linear trajectories of attack of the Ba atom on the halogen molecule might be expected to lead to reaction without assuming intermediate configurations which felt the presence of this well; in terms of the electron transfer model, these reactive trajectories, at least, would be expected to resemble those characteristic of alkali reactions. Furthermore, the metal atom (alkali or alkaline earth) cannot transfer its totally symmetric valence electron into the vacant σ_u orbital (the lowest unfilled orbital) of X_2 in the case of the broadside approach along the C_{2v} symmetry axis because these two orbitals transform as different irreducible representations of the C_{2v} point group; this symmetry restriction is likely to favor the co-linear approach trajectory in reactive collisions.²⁰

Moreover, even if the BaX_2 well were sampled in a significant fraction of the reactive trajectories, a crude RRK estimate indicates that, owing to the large reaction exoergicity, the lifetime of the complex would ^{probably} not exceed its rotational period.

The ionization potentials of Ba, Sr, Ca, and Mg are 5.2, 5.7, 6.1, and 7.6 eV. respectively. Thus, reactions of this family of atoms should show the transition from a reaction forming an ionic bond, where the potential surface exhibits long-ranged reactant attraction due to an electron transfer, to a reaction forming a covalent (more precisely, less ionic) bond, where the potential surface leading from reactants to products is more short-ranged and is, presumably, traversed more quickly. In view of this, it is perhaps surprising that the CM reactive cross sections given in Table II and Figs. 1, 4, and 5 don't exhibit more variation for changing reactants. The stochastic MgCl angular distribution from $Mg + Cl_2$ which is shown in Fig. 4 is striking; this reaction especially warrants further study, with product velocity measurements, to quantitatively determine the CM cross section. While the wide-angle isotropic product scattering is likely to arise from small impact parameter collisions, the sharp forward spike in the product angular distribution for this reaction is suggestive of a spectator stripping mechanism. Although the true reaction trajectories are unlikely to be quite this simple, the spectator stripping model might approximate them because of rapidly acting forces in the reaction. Similar ideas have been advanced²¹ in discussion of the forward product scattering seen in the $Cl + Br_2$ reaction.

ACKNOWLEDGEMENT

This work was supported by the Atomic Energy Commission through the Lawrence Berkeley Laboratory. Partial support from the Committee on Research of the University of California at Berkeley is also gratefully acknowledged.

REFERENCES

1. A recent review of crossed beams kinetics studies is given in: J.L. Kinsey, MTP International Review of Science, edited by J.C. Polanyi (Butterworths, London, 1972), Physical Chemistry Series One, Vol. 9, Chap. 6.
2. S.A. Edelstein and P. Davidovits, J. Chem. Phys. 55, 5164 (1971).
3. This work is referenced in C.A. Mims, S.-M. Lin, and R.R. Herm, to be published. Other, more recent studies, include: A. Schultz, H.W. Cruse, and R.N. Zare, J. Chem. Phys. 57, 1354 (1972) (laser induced fluorescence study); and M. Menzinger, Univ. of Toronto, private communication (chemiluminescence study).
4. J.A. Haberman, K.G. Anlauf, R.B. Bernstein, and F.J. Van Itallie, University of Wisconsin Theoretical Chemistry Institute Report No. WIS-TCI-482X, Madison, Wisc., July, 1972.
5. C.D. Jonah and R.N. Zare, Chem. Phys. Letters 9, 65 (1971).
6. (a) C.A. Mims, Ph.D. thesis, University of California, Berkeley, California, 1972; (b) S.-M. Lin, Ph.D. thesis, University of California, Berkeley, California, 1972.
7. I. Estermann, O.C. Simpson, and O. Stern, Phys. Rev. 71, 238 (1947).
8. J.C. Whitehead, D.R. Hardin, and R. Grice, Mol. Phys. 23, 787 (1972).
9. K.T. Gillen, A.M. Rulis, and R.B. Bernstein, J. Chem. Phys. 54, 2831 (1971).

10. This stochastic analysis of measured LAB angular distributions was pioneered in E.A. Entemann, Ph.D. thesis, Harvard University, Cambridge, Massachusetts, 1967. The $T(\theta)$ function employed here is a special case of the general function used by Entemann.
11. The actual calculation of $I_{\text{LAB}}(\theta)$ using the SRE analysis proceeds by selecting a single value of u and eliminating the integration over v as well as altering the Jacobian factor in Eq. (2); further details are given in Ref. 10.
12. T.T. Warnock, R.B. Bernstein, and A.E. Grosser, *J. Chem. Phys.* 46, 1685 (1967).
13. J.H. Birely, R.R. Herm, K.R. Wilson, and D.R. Herschbach, *J. Chem. Phys.* 47, 993 (1967).
14. R. Grice and P.B. Emedocles, *J. Chem. Phys.* 48, 5352 (1968).
15. D.D. Parrish and R. R. Herm, *J. Chem. Phys.* 51, 5467 (1969).
16. N.C. Blais, *J. Chem. Phys.* 49, 9 (1968).
17. P.J. Kuntz, M.H. Mok, and J.C. Polanyi, *J. Chem. Phys.* 50, 4623 (1969).
18. W.B. Miller, S.A. Safron, and D.R. Herschbach, *Disc. Faraday Soc.* 44, 108 (1967); G.H. Kwei, A.B. Lees, and J.A. Silver, *J. Chem. Phys.* 55, 456 (1971).
19. D.D. Parrish and R.R. Herm, *J. Chem. Phys.* 54, 2518 (1971).
20. P.B. Foreman, G.M. Kendall, and R. Grice, *Mol. Phys.* 23, 127 (1972).
21. N.C. Blais and J.B. Cross, *J. Chem. Phys.* 52, 3580 (1970).

Table I. Experimental beam conditions.^a

Collision partners	Alkaline earth atom beam		Halogen molecule beam	
	source conditions temperature ^b	speed distribution ^c α_1	source conditions temperature	"flow speed" ^c α_2
Br ₂ + Ba	1060	0.3 3.1	1.1 340	4-5 1.4
Br ₂ + Sr	960	0.4 3.7	1.3 340	2.5-3.3 1.4
Br ₂ + Ca	1020	0.3 5.8	1.9 350	3-4 1.4
Br ₂ + Mg	820	0.3 6.7	2.2 340	~4 1.4
Cl ₂ + Ba	1050	0.3 3.1	1.1 340	2 1.7
Cl ₂ + Sr	960	0.4 3.7	1.3 330	~4 2.0
Cl ₂ + Ca	1010	0.3 5.8	1.9 360	3.0-3.5 2.0
Cl ₂ + Mg	820	0.3 6.7	2.2 340	2-4 1.7-2.0

^a Temperatures are given in °K, pressures in Torr, and speeds in 100 m/sec.

^b Obtained from vapor pressures of the alkaline earths given in: J.L. Margrave, Characterization of High Temperature Vapor, John Wiley and Sons, Inc., New York, 1967.

^c Taken from data given in Ref. 6a; symbols refer to parameters in Eq.(1).

Table II. Results of data analysis of the $M + X_2 \rightarrow MX + X$ reactions.^a

Reactants	Energetics			Stochastic Analysis ^e			SRE Analysis	
	E ^b	W ^c	ΔD_0^d	H ₁	C ₁	u ₁	\bar{E}, f	\bar{E}, f
Br ₂ + Ba	2.5	1.1	55	20°	.08	3.2	4.8	5.5
Br ₂ + Sr	2.4	1.1	35	27°	.20	4.3	5.6	5.0
Br ₂ + Ca	2.7	1.1	45	20°	.12	6.0	6.3	6.5
Br ₂ + Mg ^g	2.3	1.1	29	15°	.15	5.0	3.5	4.8
Cl ₂ + Ba	2.1	0.9	48	35°	.15	2.3	3.1	3.5
Cl ₂ + Sr	2.2	0.9	39	35°	.15	3.5	3.5	3.5
Cl ₂ + Ca	2.6	0.9	37	35°	.25	5.5	4.2	4.0
Cl ₂ + Mg ^g	2.2	0.9	17	10°	.06	4.5	1.9	3.5

^a Energies are given in kcal/mole and speeds in 100 m/sec.

^b E is the characteristic initial relative kinetic energy, calculated for the most probable (number density distribution) beam speed.

^c W is the internal (rotational and vibrational) energy of the halogen molecule.

This could be an overestimate if the internal degrees of freedom relax in the beam expansion.

Table II Cont'd.

- ^d $\Delta D_0 = D_0(\text{MX}) - D_0(\text{X}_2)$. D_0 for Cl_2 and Br_2 taken from: R.J. Leroy and R.B. Bernstein, *Chem. Phys. Letters* 5, 42 (1970). D_0 for MCl taken from: D.L. Hildebrand, *J. Chem. Phys.* 52, 5751 (1970); ± 3 estimated uncertainties. D_0 for MBr taken from: A.G. Gaydon, *Dissociation Energies and Spectra of Diatomic Molecules* (3rd Ed.) (Chapman and Hall, Ltd., London, 1968); ± 15 estimated uncertainties.
- ^e H_1 , C_1 , and u_1 are parameters in Eqs. (4a) and (4b). The θ_1 parameter of Eq. (4a) was 0° for all reactions.
- ^f \bar{E}' is the most probable product recoil energy, obtained from the position of the peak in the $P(E')$ function.
- ^g The stochastic analysis can fit the Mg reactions data almost as well for even narrower $T(\theta)$ curves. For example, adequate fits are provided by: $H_1 = 5^\circ$, $C_1 = .05$, $u_1 = 4.3$ for $\text{Mg} + \text{Br}_2$; and $H_1 = 5^\circ$, $C_1 = .03$, $u_1 = 4.5$ for $\text{Mg} + \text{Cl}_2$.
-

Table III. Fraction of product MX scattered into forward CM hemisphere, Q_F .

	Br ₂ reactions				Cl ₂ reactions			
	Mg	Ca	Sr	Ba	Mg	Ca	Sr	Ba
Q_F , stochastic	0.56	0.62	0.62	0.67	0.58	0.64	0.71	0.71
Q_F , SRE	0.63	0.67	0.68	0.73	0.67	0.65	0.71	0.70
MX ₂ Geometry ^a	ℓ	ℓ	ℓ	b	ℓ	ℓ	b	b

^a MX₂ geometry; ℓ for linear and b for bent; data taken from L. Wharton, R.A. Berg, and W. Klemperer, J. Chem. Phys. 39, 2023 (1963).

FIGURE CAPTIONS

Fig. 1. The data points show the measured LAB angular distribution from the $\text{Ba} + \text{Cl}_2$ reaction. The solid, short-dashed, and dot-dashed CM angular distributions were combined with the solid CM recoil energy distribution (all shown in the upper panel) to calculate the corresponding BaCl LAB angular distributions shown in the lower panel; note that the dot-dashed and solid CM angular distributions are identical for $\theta \leq 90^\circ$. Calculations for the short-dashed and dot-dashed CM angular distributions with other forms of $P(E')$ are in equally poor agreement with the data. The long-dashed LAB BaCl angular distribution shown in the lower panel was calculated from the corresponding angular distribution in the upper panel by assuming a single product recoil energy of 3.5 kcal/mole. Also shown are: (1) angular profiles of the two beams; (2) calculated distribution in \vec{C} (dotted curve); and (3) a LAB \leftrightarrow CM transformation diagram drawn for the most probable beam speeds. The circles indicate the BaCl recoil speed for some possible product recoil energies, E' (kcal/mole).

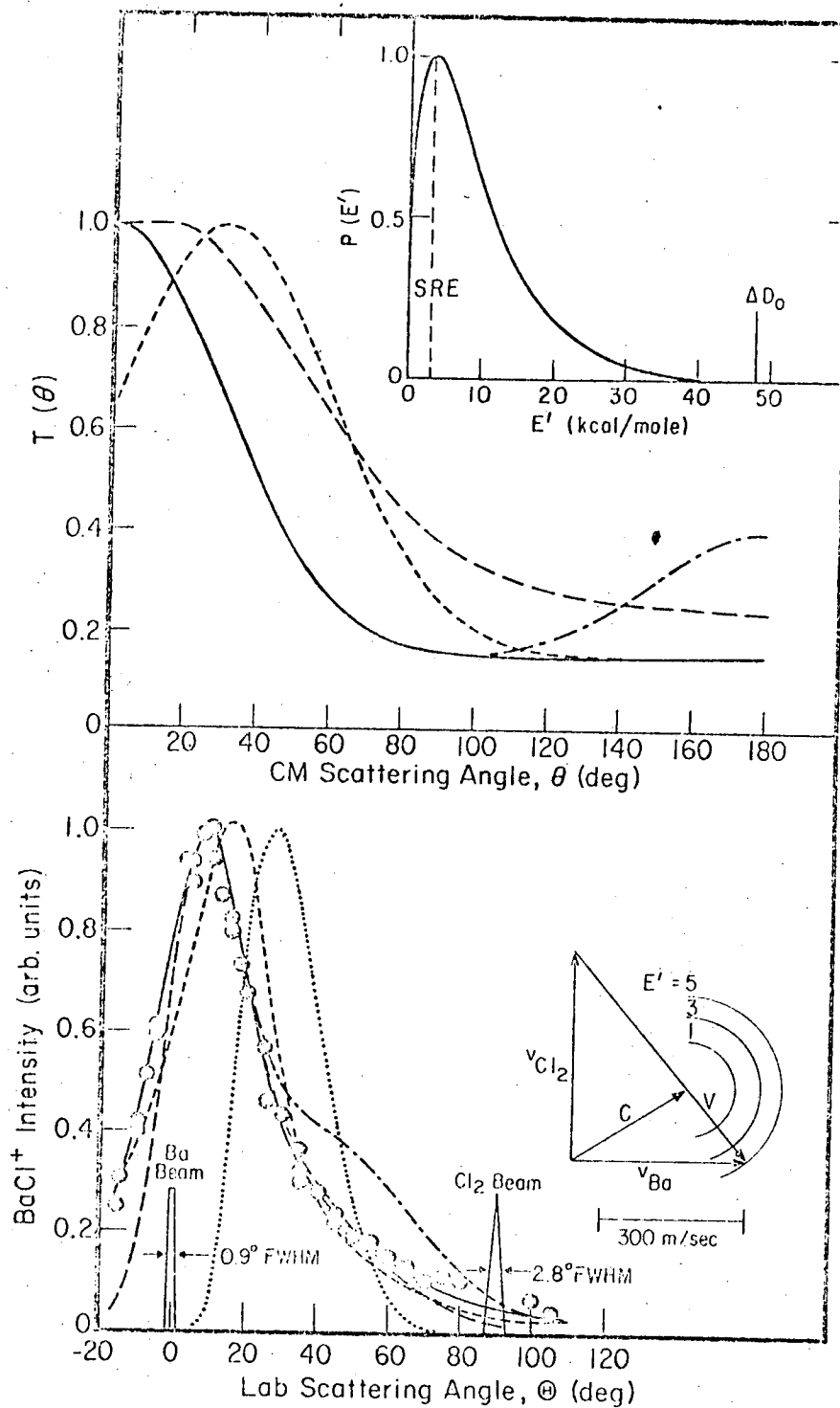
Fig. 2. The data points show the measured LAB angular distributions from the Sr, Ca, and Mg + Cl_2 reactions; different data symbols indicate experiments run on different apparatus pumpdowns. The solid and long-dashed curves are, respectively, the stochastic and SRE fits provided by CM

angular distributions shown in Fig. 4 and recoil speed distributions given in Table II. The short-dashed curves show calculated distributions in \vec{C} .

Fig. 3. Fits to the measured data points, provided by CM cross sections given in Fig. 5 and Table II, for the Ba, Sr, Ca, and Mg + Br₂ reactions. Conventions are as described for Fig. 2.

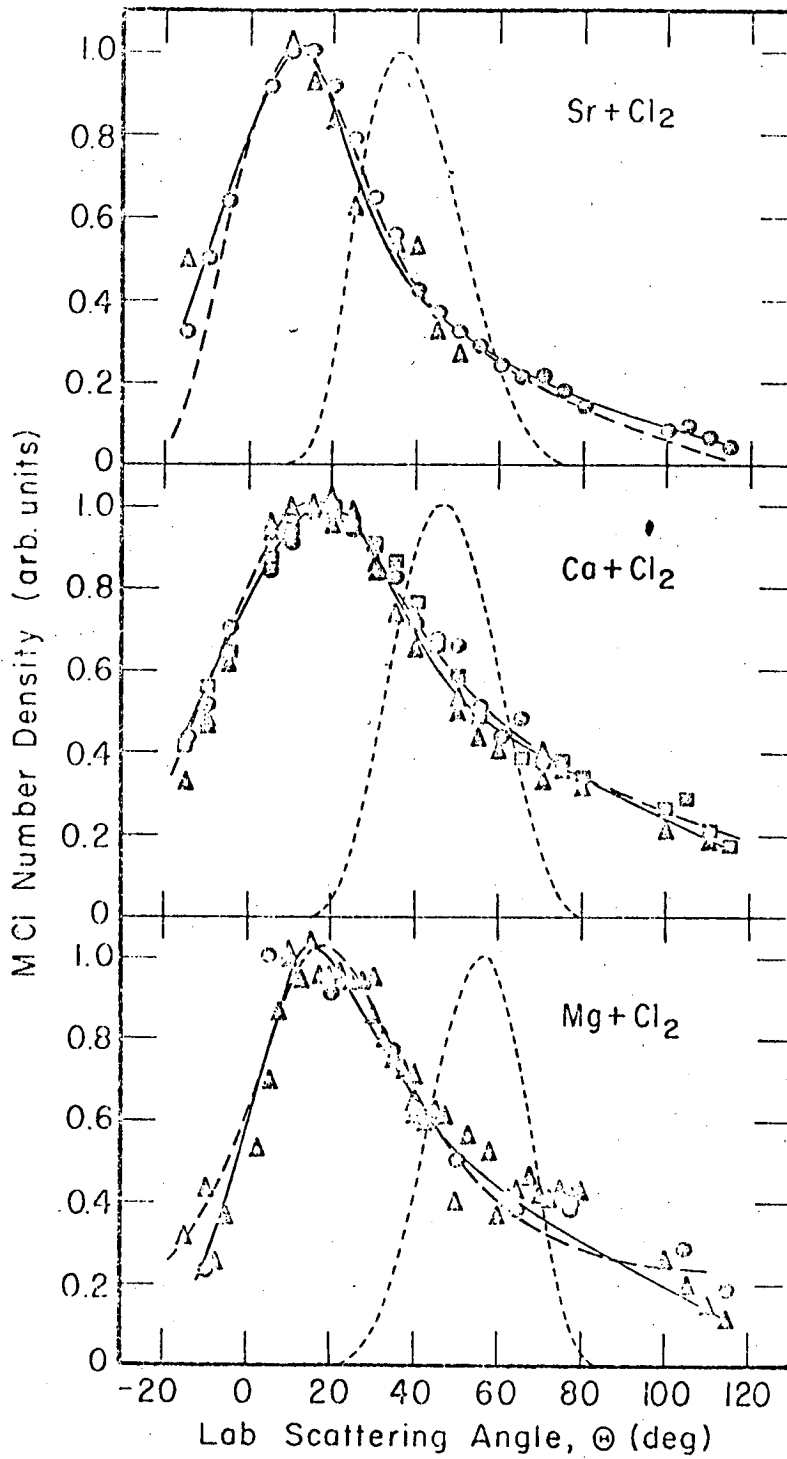
Fig. 4. Stochastic (solid curves) and SRE (dashed curves) MCl product CM angular distributions which provide the fits to the data shown in Fig. 2.

Fig. 5. Stochastic (solid curves) and SRE (dashed curves) MBr product CM angular distributions which provide the fits to the data shown in Fig. 3.



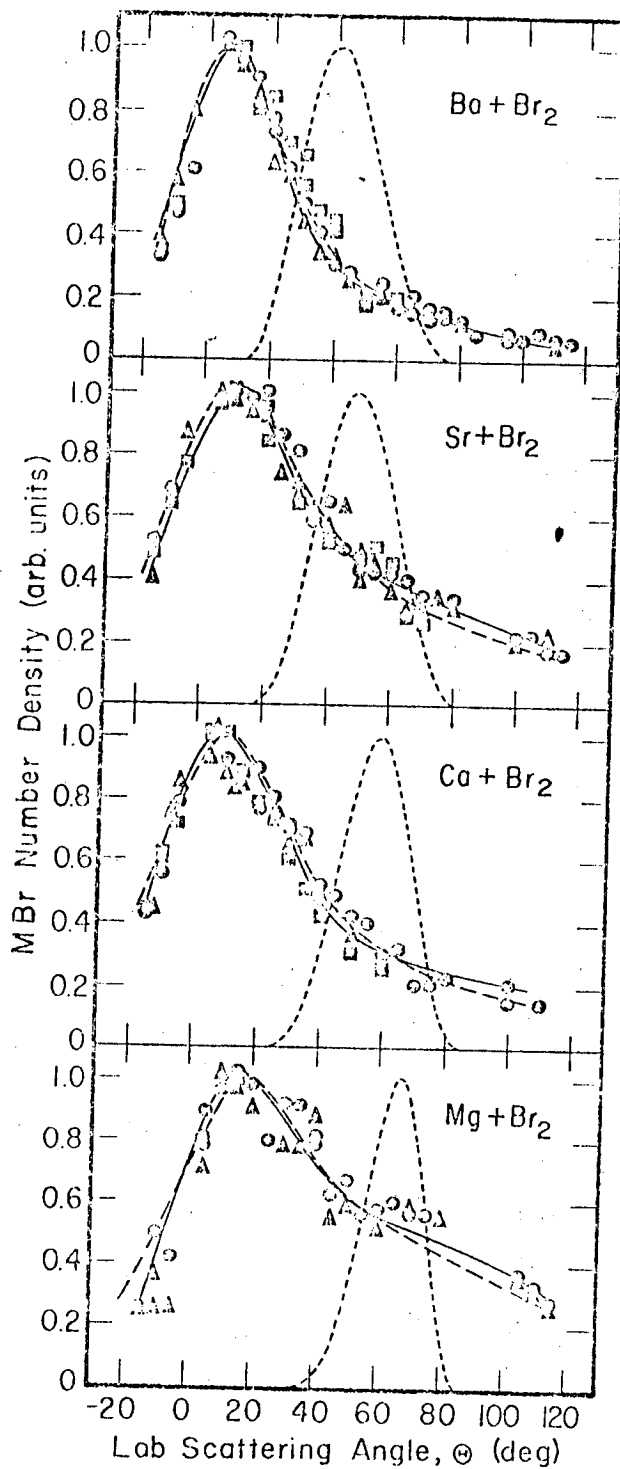
XBL 727-6730

Fig. 1



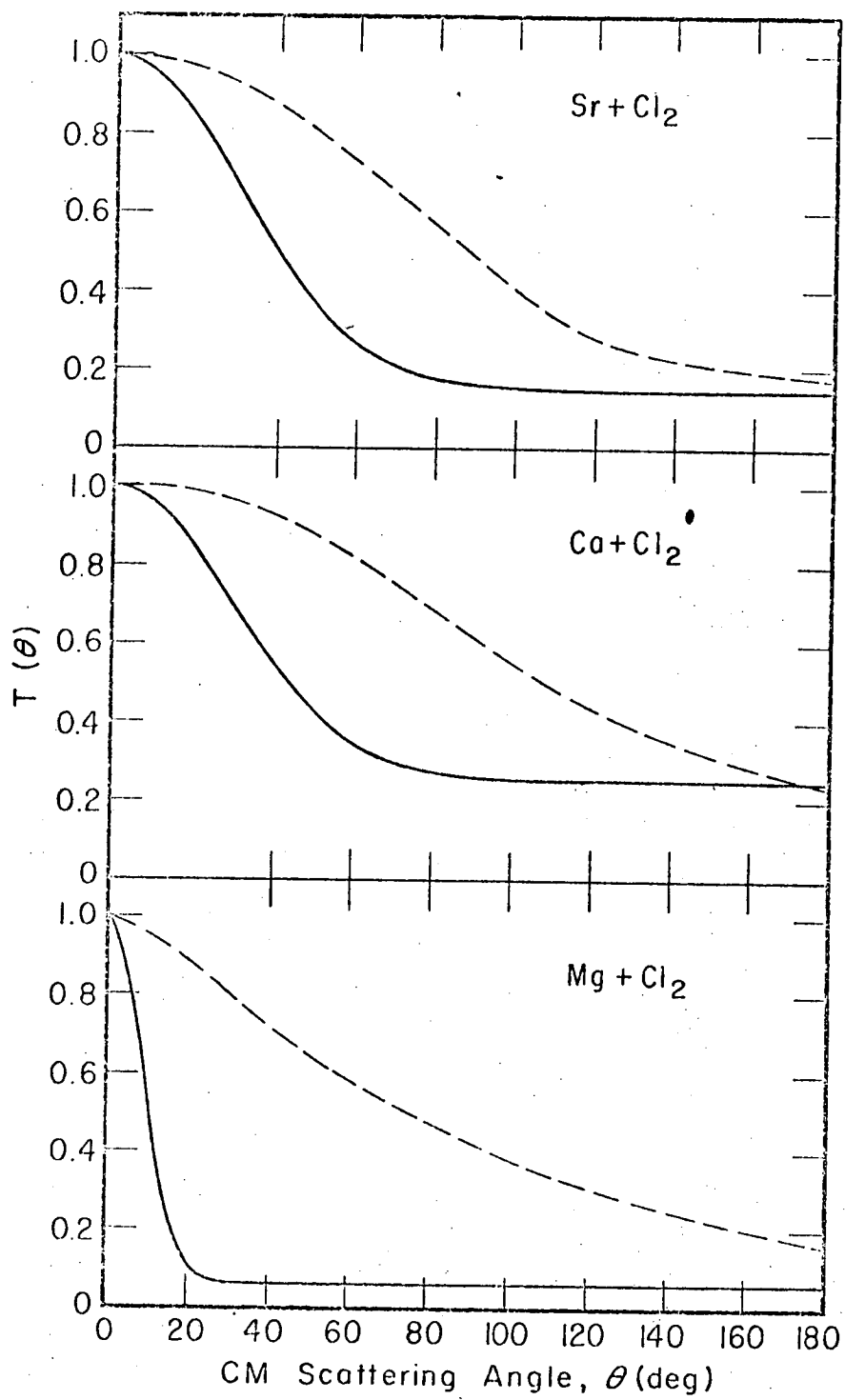
XBL 728-67 31

Fig. 2



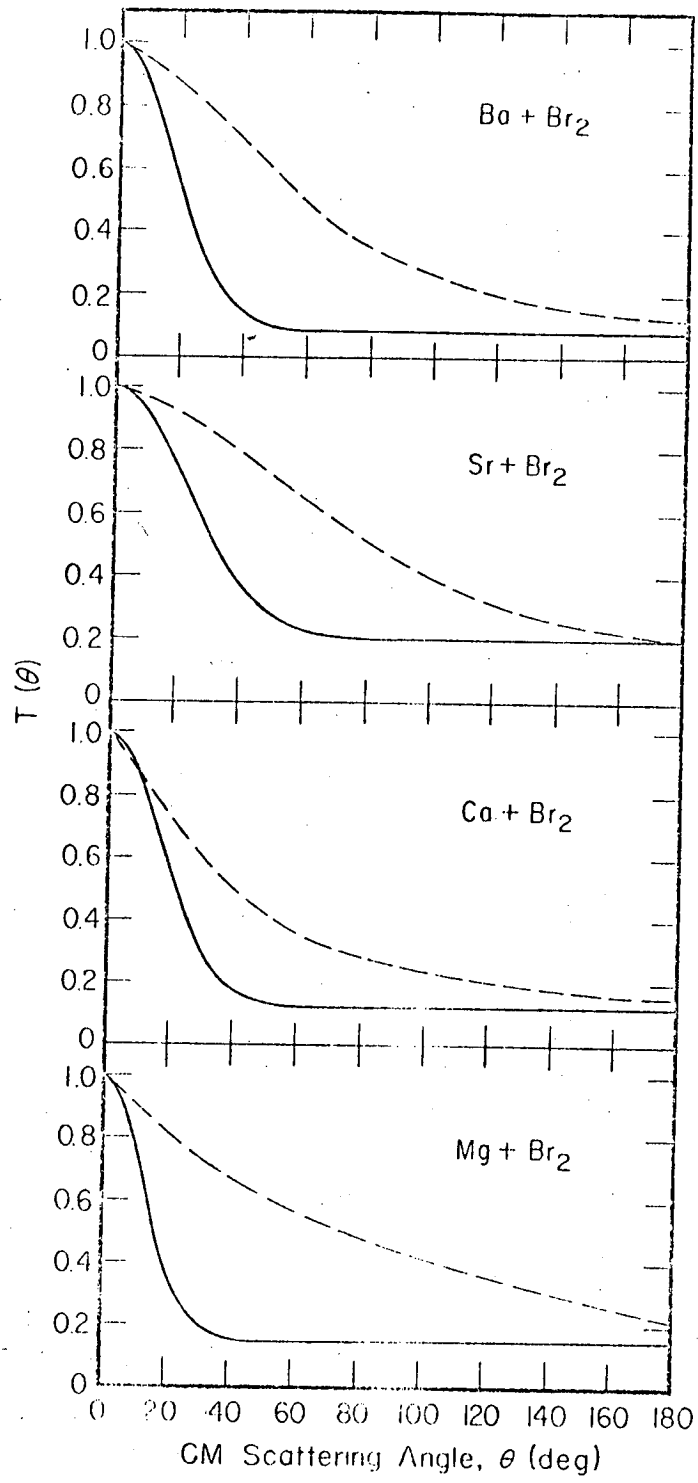
XBL 728-6732

Fig. 3



XBL728-6754

Fig. 4



xBL728-6755

Fig. 5

LEGAL NOTICE

This report was prepared as an account of work sponsored by the United States Government. Neither the United States nor the United States Atomic Energy Commission, nor any of their employees, nor any of their contractors, subcontractors, or their employees, makes any warranty, express or implied, or assumes any legal liability or responsibility for the accuracy, completeness or usefulness of any information, apparatus, product or process disclosed, or represents that its use would not infringe privately owned rights.

TECHNICAL INFORMATION DIVISION
LAWRENCE BERKELEY LABORATORY
UNIVERSITY OF CALIFORNIA
BERKELEY, CALIFORNIA 94720